

Investigation of the Peptide Adsorption on ZrO₂, TiZr, and TiO₂ Surfaces as a Method for Surface Modification

Tina Micksch,[†] Nora Liebelt,[†] Dieter Scharnweber,^{*,§,‡} and Bernd Schwenzer^{†,‡}

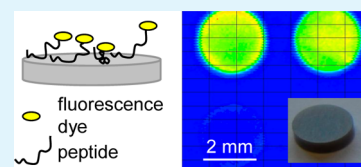
[†]Lehrstuhl für Allgemeine Biochemie, Technische Universität Dresden, Bergstr. 66, Dresden, Saxony 01069, Germany

[§]Max-Bergmann-Zentrum für Biomaterialien, Technische Universität Dresden, Budapester Str. 27, Dresden, Saxony 01069, Germany

S Supporting Information

ABSTRACT: Specific surface binding peptides offer a versatile and interesting possibility for the development of biocompatible implant materials. Therefore, eight peptide sequences were examined in regard to their adsorption on zirconium oxide (ZrO₂), titanium zircon (TiZr), and titanium (c.p. Ti). Surface plasmon resonance (SPR) measurements were performed on Ti coated sensor chips to determine the kinetics of the interactions and kinetic rate constants (k_{on} , k_{off} , K_{D} , and R_{max}). We also investigated the interactions which are present in our system. Electrostatic and coordinative interactions were found to play a major role in the adsorption process. Four of the eight examined peptide sequences showed a significant adsorption on all investigated materials. Moreover, the two peptides with the highest adsorption could be quantified (up to 370 pmol/cm²). For potential biomaterials applications, we proved the stability of the adsorption of selected peptides in cell culture media, under competition with proteins and at body temperature (37 °C), and their biocompatibility via their effects on the adhesion and proliferation of human mesenchymal stem cells (hMSCs). The results qualify the peptides as anchor peptides for the biofunctionalization of implants.

KEYWORDS: peptide, adsorption, biocompatibility, titanium, zirconium, surface modification



1. INTRODUCTION

The design of novel biomaterials has so far been limited to the existence and number of functional groups for the covalent linkage of biomolecules. A versatile and widely applicable approach for the functionalization of materials is offered by the specific recognition and adsorption of peptides. Specifically binding peptides have the potential to act as biological anchor for biomolecules on inorganic (e.g., metals) and organic (e.g., polymers) materials.

A group of mussel adhesive peptides (MAPs) was shown to adsorb strongly on a variety of inorganic materials (e.g., Au, Fe (III) compounds, and Ag).¹ Dalsin et al. used MAPs and their component 3,4-dihydroxyphenylalanine (DOPA) as anchor for linear monomethoxy-terminated poly(ethylene glycol) (PEG) to adapt new properties on Au and Ti surfaces² and achieved nonfouling surfaces with a 98% decreased cell attachment. Lee, Lee, and Messersmith combined the DOPA group for the modification of polymers with the structure of the foot pads of geckos to form adhesive surfaces.³

The mechanism of the adhesion of MAPs to inorganic materials has still not been fully understood, but Yu could prove that DOPA is essential for adhesion.⁴ Ooka et al. have focused on surface enhanced Raman spectroscopy (SERS) to determine the interactions between MAPs and Au. They assumed the deprotonated catechol oxygens of DOPA and primary amino groups to be responsible for the adsorption.¹ Additionally, they have suggested that conformational properties, especially the orientation of DOPA, have great influence on the adsorption on Au.

A further application of anchor peptides is the design of sensor surfaces. Kacar et al. used an Au binding peptide for the immobilization of the enzyme alkaline phosphatase (ALP).⁵ They fused the peptide in up to 9-fold repetition to the N-terminus of ALP and expressed it in *E. coli* cells. The 5-fold presentation of the binding peptide presented the highest stability.

For medical applications, the modification of materials such as Ti by the immobilization of biologically active molecules (e.g., antibiotics, arginine–glycine–aspartic acid (RGD) peptides, or growth factors) is of great importance. Kashiwagi et al. used the 3-fold presentation of the Ti binding sequence RKLPGA to immobilize reversibly bone morphogenetic protein 2 (BMP-2) on the Ti surface.⁶ After the adsorption of BMP-2 by the anchor peptide, the biological activity could be maintained contrary to the direct adsorption of BMP-2 resulting in little activity. The group of Meyers used polystyrene (PS) binding peptides to link the biologically active cell-binding sequence RGD on the surface.⁷ Human umbilical vein endothelial cells (HUVEC) interacted with the RGD-modified PS showing about a 9-fold increase in cell seeding density compared with the unmodified PS.

Although numerous attempts have been made to use peptides, found by phage display or cell surface display on the correspondent material, as a robust and versatile anchor for the surface modification, the mechanism of the peptide

Received: February 8, 2014

Accepted: April 15, 2014

Published: April 15, 2014

Table 1. Sequences, Molecular Weight, and References of the Examined Peptides

name	sequence	molecular weight	references
Pep1	HKKPSKSG-EDA-Btn x TFA	1,136.4	Chen et al. 2006
Pep1Dy557	HKKPSKSG-EDA-Dy557 x TFA	1,680.1	Chen et al. 2006
Pep2	RKLPDAPGGRKLPDAPGG-G-EDA-Btn x TFA	2,127.5	Sano and Shiba 2003
Pep3	CGPGMEFGRKRDRVNGP-G-EDA-Btn x TFA	2,201.6	Gronewold et al. 2009
Pep4	N-Acetyl-pSGG-K(Ahx-Btn)-GGpS-Amid x TFA	1,089.0	
Pep5	SHKHGGHKGHGGHKGSSGK-G-EDA-Btn x TFA	2,282.5	Khoo et al. 2009
Pep5Dy557	SHKHGGHKGHGGHKGSSGK-G-EDA-Dy557	2,826.2	Khoo et al. 2009
Pep6	HKHGGHKGHGGHKGHGG-G-EDA-Btn x TFA	1,893.1	Khoo et al. 2009
Pep7	pSGGpSGGpSGGpSGG-G-EDA-Btn x TFA	1,468.1	
Pep8	YKVPQLEIVPNpSAEER-G-EDA-Btn x TFA	2,277.5	Larsen et al. 2005

adsorption on inorganic surfaces is still not fully understood. Despite investigations regarding the reasons of the adsorption or the classification of particular peptides or amino acids, only little general information has been found.⁸

Chen et al. identified the alkaline peptide HKKPSKS (Pep1) to adsorb on the oxides TiO₂ and SiO₂ at pH 7.5.⁹ They proved the three lysine residues to be crucial for adsorption by point mutation and assumed electrostatic interactions to be the reason for the adsorption because of the strong pH dependence of the adsorption.¹⁰

Sano and Shiba determined the surface density of Pep2 (5 · 10⁴ pfu (phage forming units)) on TiO₂ with quartz crystal microbalance (QCM) in comparison to unspecific adsorption of bovine serum albumin (BSA) (2 · 10² pfu).¹¹ The authors assumed the hydrophobic interactions to be less important for Pep2 as its adsorption was not affected by the ionic strength. They identified the RKLPDA sequence to be crucial for the adsorption by amino acid replacement and found the peptide to adsorb on Ag and Si surfaces but not on Au, Cr, Pt, Sn, Zn, Cu, and Fe surfaces. For our studies, we selected the peptide with the 2-fold presentation of the binding sequence RKLPDA separated by two glycine residues ensuring the necessary flexibility.

Gronewold et al. incorporated peptide motifs into thioredoxin and presented it on the surface of *E. coli* cells to find selective TiO₂ binding peptides.¹² With a surface acoustic wave sensor, the adsorption on a TiO₂ coated silicon wafer could be determined. The peptide CGPGLVLETVGSARGPC showed a dissociation constant *K_D* of 81 nM and a density of 0.52 ng/cm², though Pep3 (CGPGMEFGRKRDRVNGP) was found to have an even higher surface density of 1.42 ng/cm².

Khoo et al. searched for peptides specifically adsorbing to the Ti6Al4V alloy.¹³ They identified the peptide SHKHVPVTP-RFFVVESK and proved the HKH motif to be essential for the adsorption. Therefore, peptides with different numbers of separated HKH motifs were examined. Pep5 (SHKHGGHKGHGGHKGSSGK) was found to adsorb with the highest amount of 102 pmol/cm² (*K_D* = 35 nM). The conjugation of Pep5 with PEG allowed for an adsorption with a density of 95 pmol/cm². In the present study, we investigated Pep5 with the 3-fold presentation of the binding motif HKH as well as Pep6 as simplification of Pep5 without the serine residues.

The enrichment of phosphorylated peptides with ZrO₂ and TiO₂ has been accomplished by several research groups examining samples of model phosphoproteins and complex mixtures, e.g., tryptic digested α - and β -casein and ovalbumin.^{14,15} Phosphorylated peptides could be isolated from aqueous solution in the presence of nonphosphorylated

peptides 2 orders of magnitude higher. The high affinity of ZrO₂ and TiO₂ to phosphorylated peptides may result from a bidentate-bridging coordination of the phosphate group to TiO₂ and ZrO₂ particles, respectively. The influence of the number of phosphorylation sites on the affinity of TiO₂ and ZrO₂ for phosphorylated peptides could not be clarified because the detection was done qualitatively by mass spectrometry. Pep3, a symmetric peptide with two phosphoserine residues with blocked terminal groups, and Pep7 consisting of four separated phosphoserine residues were designed as model peptides to examine the influence of phosphorylated amino acids on the peptide adsorption. Larsen et al. developed a highly selective enrichment procedure for phosphorylated peptides based on TiO₂ micro columns and peptide loading in 2,5-dihydroxybenzoic acid (DHB).¹⁴ DHB decreased the binding of nonphosphorylated peptides to TiO₂ and retained its high binding affinity for phosphorylated peptides and therefore increased the selectivity of the enrichment. In their studies, they identified Pep8 (α -S1-casein (119–134)) to adsorb specifically to TiO₂.

The aim of this work was to identify different specific binding peptides for typical implant materials: zirconium oxide (ZrO₂), titanium zircon (TiZr), and titanium (c.p. Ti). We intended to compare the promising anchor peptides from literature and to investigate the adsorption process and the influencing factors to understand the adsorption in greater detail. Therefore, we selected peptides which were reported to adsorb on either ZrO₂, Ti alloys, or TiO₂ (Table 1) proven by phage and cell surface display. TiO₂ binding peptides were used because Ti naturally forms an oxide layer on the surface.

2. EXPERIMENTAL DETAILS

2.1. Materials and Chemicals. Dy557-NHS (Dyomics GmbH, Jena, Germany), Dulbecco's modified Eagle medium (DMEM) (Biochrom AG, Berlin, Germany), fetal calf serum (FCS) (Lonza Ltd., Basel, Switzerland), horseradish peroxidase streptavidin conjugate (HRP-SA) (Sigma-Aldrich, MDL: MFCD00132387), lactate dehydrogenase (LDH) Cytotoxicity Detection Kit (TaKaRa Bio Inc., France), disc-shaped zirconium oxide (ZrO₂), titanium–zirconium alloy (TiZr) (13–17% Zr) and titanium (Ti) samples with the SLActive surface (*d* = 5 mm, *h* = 1 mm) (both from Institute Straumann AG (Basel, Switzerland)), and SIA Kit Au (GE Healthcare Europe GmbH, Freiburg, Germany) were used. All buffers were made from p.a. grade chemicals supplied by Merck KGaA (Darmstadt, Germany) and autoclaved before use. Buffer compositions are as follows: HBS-EP (0.01 M Hepes (pH 7.4), 0.15 M NaCl, 3 mM EDTA, 0.005% surfactant P20) (GE Healthcare Europe GmbH, Freiburg, Germany), phosphate buffered saline (PBS) pH 7.4 (6.7 mM phosphate, 154 mM NaCl), citrate buffered saline pH 3, acetate buffered saline pH 5, phosphate buffered saline pH 7.4, and borate buffered saline pH 9 and 11 (25 mM buffer, 75 mM NaCl).

2.2. Peptides. The sequences of the eight peptides with C-terminal biotinylation and two peptides with Dy557 used, investigating the adsorption, are listed in Table 1.

The peptide syntheses were performed by Biosyntan GmbH, Berlin, Germany. The peptides were purified by high pressure liquid chromatography (HPLC) and characterized by mass spectrometry.

2.3. Peptide Adsorption. Solutions containing 10 μM peptide (Table 1) in PBS pH 7.4 were prepared freshly. The peptide solution (25 μL) was added on top of the substrates (ZrO_2 , TiZr , TiO_2) in a microtiter plate with 24 wells. After 1 h, the peptide solutions were removed and the samples were washed with 500 μL of PBS pH 7.4 for 10 min on a horizontal shaker (200 rpm).

2.4. Desorption Experiments. After peptide adsorption, desorption followed in 500 μL of variable desorption buffer on a horizontal shaker (200 rpm) for different durations.

2.5. Quantification of Adsorbed Peptides. The surface densities of adsorbed peptides were measured via a horseradish peroxidase-based (HRP) enzymatic assay adapted from Bisswanger using tetramethylbenzidine (TMB) as substrate.¹⁶ Additionally, they were examined by fluorescence measurements on the substrate surfaces (ZrO_2 , TiZr , and TiO_2) as well as in solution after complete desorption of the peptides from the substrate surface and on the TiO_2 surface with surface plasmon resonance (SPR) measurements.

2.5.1. Enzymatic Assay. Gaebler et al. developed an enzymatic assay to detect peptides adsorbed on calcium phosphate (CaP) surfaces.¹⁷ The peptides were conjugated to biotin. After the adsorption on CaP, a horseradish-peroxidase-streptavidin (HRP-SA) conjugate could bind by biotin-streptavidin interactions. The excessive HRP-SA conjugate was removed, and the enzymatic activity was determined by the 3,3',5,5'-tetramethylbenzidine (TMB) assay.

Therefore, the samples were incubated with 15 μL of 25 $\mu\text{g}/\text{mL}$ HRP-SA in PBS pH 7.4 for 30 min and afterward with 500 μL of PBS pH 7.4 for 10 min on a shaker to remove unspecifically bound HRP-SA. The substrate solution consists of a 1:1 mixture of 0.5 mg/mL TMB in DMSO and 0.06% H_2O_2 in 205 mM citrate buffer pH 4.0 and was prepared freshly each day. In microtiter plates with 96 wells, 100 μL of substrate solution was added to each sample (ZrO_2 , TiZr , or TiO_2 with 150 μL of PBS pH 7.4). After sufficient color development, the incubation was stopped by addition of 50 μL of 2 N H_2SO_4 . The extinction of 100 μL of each sample was measured at 450 and 540 nm with the BioTek ELx800. HRP densities were calculated using the defined amounts of HRP-SA (0, 0.5, 1, 2.5, 5, 10, 20 ng/well). Unspecific adsorption of HRP-SA to ZrO_2 , TiZr , and TiO_2 was estimated using reference samples.

2.5.2. Fluorescence Measurements. On the Surface. The fluorescence on the samples was measured with the fluorescence spectrometer LIMES (Laser-Induced Multi Emission Spectrometer) (Lasertechnik Berlin GmbH, Germany) with the following parameters: excitation/emission wavelength: 520 nm/570–590 nm; accumulation of shots: 20; laser repetition rate: 30 Hz.

In Solution. The adsorbed peptides were fully desorbed from the samples in 400 μL of 5 M NaCl solution on a horizontal shaker (200 rpm) for 30 min. The peptide solution was mixed equimolar with PBS. The peptide solution (300 μL) was measured in a precision cuvette made from quartz glass Suprasil (Hellma GmbH & Co. KG) with the fluorescence spectrometer F-4500 (HITACHI) with the following parameters: mode: Time Scan; excitation/emission wavelength: 460 nm/480 nm; excitation and emission wavelength slit: 5 nm; time, 200 s. The peptide densities were determined using a calibration with different peptide concentrations.

2.6. Surface Plasmon Resonance (SPR) Measurements. For interaction analysis of peptides on TiO_2 surfaces, a BIACore T100 instrument with *Evaluation Software* 2.03 was used. The SIA Kit Au was used for the coating of a sensor chip with a Ti layer (5 nm). Before use, the sensor chip was stored in buffer solution overnight to completely wet the surface. All steps were carried out in a continuous flow of HBS-EP running buffer (30 $\mu\text{L}/\text{min}$), and all buffers were degassed prior to use. The baseline was allowed to stabilize for 30 min in HBS-EP running buffer before injecting samples. Each sample was prepared in HBS-EP buffer and injected for 300 s at 30 $\mu\text{L}/\text{min}$,

followed by a 300 s dissociation phase. The sensor surface was regenerated using 5 M NaCl for 60 s. Re-equilibration between the sensor surface and running buffer was established prior to injection of the next sample by a 90 s prerun phase. The response was monitored as a function of time (sensorgram) at 25 $^\circ\text{C}$.

2.7. Proliferation Tests with Mesenchymal Stem Cells. Human mesenchymal stem cells (hMSC) (passage three, received from Universitätsklinikum Dresden) were grown in 96-well cell culture plates on the disc-shaped ZrO_2 , TiZr , and TiO_2 samples with DMEM, containing 10% FCS, 1% penicillin-streptomycin, and 2 mM L-glutamine at 37 $^\circ\text{C}$ and 7% CO_2 in a humidified incubator. Before cell seeding, all samples were prepared freshly with the respective surface conditions as described above. Subsequently, they were seeded with 1×10^4 hMSCs per cm^2 , and cell culture medium was added. Medium was changed thrice weekly. After 1, 7, and 14 days (d), cells were lysed using 1% TritonX100 PBS solution for 50 min on ice.

2.7.1. Lactate Dehydrogenase (LDH) Determination. The lysed cells were mixed with LDH Cytotoxicity Detection Kit, and the extinction was measured at 492 nm with a microplate reader.

2.8. Statistical Analyses. Data values are presented as mean ($n = 3$) \pm standard error (SE). Dixon's Q test was used to determine outliers which were not included for averaging. Differences among the samples were assessed using a student's *t* test, and *p*-values of 0.05 and below were reported as being significant.

3. RESULTS

3.1. Peptide Adsorption. 3.1.1. Quantification of the Peptide Adsorption. Eight different peptides were selected from the literature to adsorb either on ZrO_2 , Ti alloys, or TiO_2 . We investigated the peptides known to adsorb on TiO_2 as Ti naturally forms an oxide layer on the surface. To select the peptides regarding their adsorption, three methods were used (enzymatic assay and fluorescence and SPR measurements). We modified an enzymatic assay based on the interactions of peptides conjugated to biotin and the horseradish peroxidase-streptavidin (HRP-SA) conjugate for our disc-shaped ZrO_2 , TiZr , and TiO_2 samples and semiquantitatively determined the peptide adsorption on the surfaces by measuring the enzymatic activity and calibrating with defined amounts of HRP-SA in solution.¹⁷ This calibration does not reveal quantitative results because of the great difference between the activity of the enzyme in solution and the activity of the enzyme bound on the sample surface. Additionally, the streptavidin tetramer can interact with four biotin molecules as well as with four peptide molecules conjugated to biotin. Screening many peptides on different materials, this enzymatic assay can be used to determine whether the peptides adsorb or not.

The enzymatic assay proved that five of the eight examined peptides (Pep1, Pep3, Pep5, Pep6, and Pep7) adsorbed on ZrO_2 and TiZr as well as TiO_2 surfaces (Figure 1). On ZrO_2 , all peptides showed adsorption while on TiZr and TiO_2 the peptides Pep2, Pep4, and Pep8 did not adsorb in considerable amounts under the investigated conditions (100 μM biotinylated peptide in PBS pH 7.4, 2 h).

Further studies regarding the peptide concentration and incubation time revealed Pep1, Pep5, and Pep6 as the most promising peptides because they achieved the highest surface densities (Supporting Information: S-1, S-2). Examining the influence of the peptide concentration on the adsorption, we observed no change of the surface densities for peptide concentrations above 5 μM . Therefore, we used peptide concentrations of 10 μM for further investigations. Additionally, the influence of the adsorption time revealed 1 h to be sufficient for the peptide adsorption.

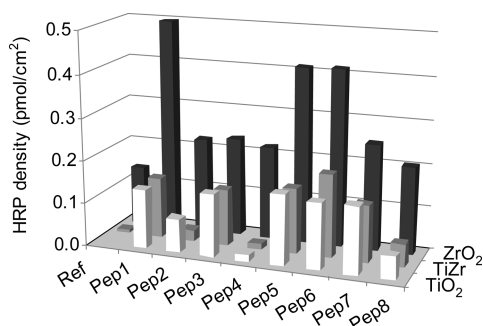


Figure 1. Peptide adsorption. Surface densities of HRP after adsorption of biotinylated peptides Pep1 to Pep8 on ZrO_2 , $TiZr$, and TiO_2 discs. Ref (Reference): Surface density of HRP without peptide. The adsorption was carried out with $100 \mu M$ peptide solution in PBS pH 7.4 for 2 h and followed by thorough rinsing of samples.

In parallel, SPR measurements have been used to investigate interactions of the peptides and the kinetics of the adsorption process with the sensor chip surface with TiO_2 coating. Unfortunately, coatings with ZrO_2 and $TiZr$ with an evenly and defined distribution were not possible. The measurements were carried out with $1 \mu M$ peptide solution because higher concentrations revealed no further increase in peptide adsorption (Supporting Information: S-3). The rating of the SPR measurements is in agreement with the results of the enzymatic assay (Figure 2). Pep5 showed the highest binding

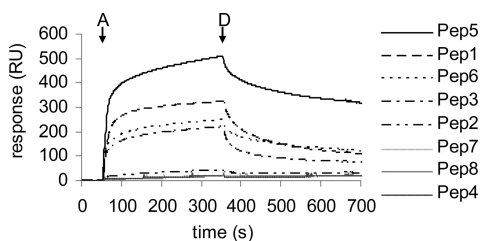


Figure 2. SPR sensorgrams of the interactions of different peptides Pep1 to Pep8 on TiO_2 at $T = 25 \text{ }^\circ C$. Sensorgrams were run at the concentrations, $1 \mu M$ in HBS-EP pH 7. The flow rate was $30 \mu L/min$. Arrow A represents the starting point of the sample injection or the beginning of the association phase (300 s). Arrow D represents the beginning of the dissociation phase (300 s). The peptides in the legend were ranged according to their response.

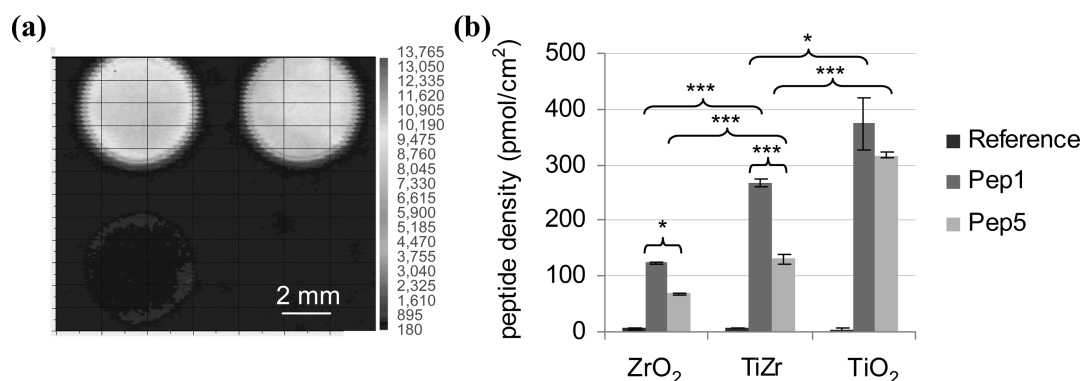


Figure 3. Peptide adsorption: Adsorption was carried out with $10 \mu M$ peptide solution in PBS pH 7.4 for 1 h, followed by thorough rinsing of samples. (a) Fluorescence image of ZrO_2 (below, left), with Pep1Dy557 (above, right) and Pep5Dy557 (above, left), dried after the adsorption. (b) Fluorescence measurements in solution: Surface densities of peptides after adsorption of Pep1/Pep5Dy557 on ZrO_2 , $TiZr$, and TiO_2 discs and desorption in 5 M NaCl (* $p < 0.05$, *** $p < 0.001$).

response of the examined peptides on the TiO_2 surface with 550 response units (RU) followed by Pep1, Pep6, and Pep3 with responses of 350 RU, 280 RU, and 240 RU, respectively. Also the low adsorption of Pep2, Pep4, Pep7, and Pep8 was proven by the SPR measurements.

The surface density of the peptides on the SPR chip was semiquantitatively estimated by the molecular mass of the peptide and the assumption that $1 \text{ RU} \approx 1 \text{ pg/mm}^2$. When the surface densities of the adsorbed peptides were examined, Pep1 showed the highest amount (30 pmol/cm^2) prior to Pep5 (24 pmol/cm^2), Pep6 (15 pmol/cm^2), and Pep3 (11 pmol/cm^2). As this assumption is normally used for Au coated sensor chips, the coating with TiO_2 might have an influence on this correlation.

To further prove the calculated values, we used fluorescence measurements after desorption to investigate the surface densities of Pep1 and Pep5 on the three materials as they revealed the highest adsorption so far (with $10 \mu M$ peptide solutions). The fluorescence image of the whole sample disc showed an even distribution of the peptides Pep1 and Pep5 (Figure 3a). The surfaces were homogeneously covered by peptides without any uncoated regions. A slight increase of the fluorescence was noticed at the edge of the discs. To eliminate background influences of the material in the quantitative analysis, the peptides with fluorescence marker Dy557 were desorbed from the surface by 5 M NaCl solution prior to quantification. SPR measurements revealed this solution as sufficient to completely remove the peptides from the TiO_2 surface. The fluorescence of the buffered solution was measured, and the amount of peptide was determined by a calibration. The fluorescence measurements showed surface densities of the adsorbed peptides Pep1 and Pep5 in the range of about 70 to 370 pmol/cm^2 (Figure 3b). The surface densities of the adsorbed peptides increased from ZrO_2 to $TiZr$ to TiO_2 . The smaller peptide Pep1 showed systematically higher surface densities than the larger peptide Pep5 on all of the three materials.

3.1.2. Kinetics of the Peptides Adsorption. The kinetics of the peptide interactions with the TiO_2 surface were investigated with SPR measurements to characterize the adsorption and desorption process as well as the stability of the peptides (Figure 2). The curves consist of the injection of the sample for 300 s and afterward the injection of buffer for 300 s. Especially Pep1, Pep3, Pep5, and Pep6 adsorbed very fast and the surface

was saturated within 100 s. The peptides reached nearly stable values after a 300 s desorption. The adsorption and desorption curves showed the best fitting using a Langmuir 1:1 approach. The Langmuir approach is based on the assumption of the adsorption of a monomolecular layer on a homogeneous surface and thus equivalent binding sites as well as the independence of the adsorption from the occupancy of nearby binding sites.¹⁸ Thus, we assumed a monolayer adsorption of the peptides on the sample surface and therefore a well-defined covering.

Using the 1:1 approach, the association and dissociation rates were derived from the SPR measurements (Table 2). The

Table 2. Kinetic Rate Constants (k_{on} and k_{off}) and Equilibrium Dissociation Constants (K_{D}) for the Interaction of Peptides with TiO_2 after Fitting with BIAcore Evaluation Software 2.03 Applying a 1:1 Binding Model

peptide	k_{on} (1/M·s)	k_{off} (1/s)	K_{D} (nM)	R_{max} (RU)
Pep1	$1.15 \cdot 10^5$	$6.24 \cdot 10^{-3}$	52.4	342
Pep3	$1.05 \cdot 10^5$	$1.28 \cdot 10^{-2}$	123	228
Pep5	$1.20 \cdot 10^5$	$1.45 \cdot 10^{-3}$	12.3	505
Pep6	$0.43 \cdot 10^5$	$3.02 \cdot 10^{-3}$	70.0	273

kinetic rate constants of Pep2, Pep4, Pep7, and Pep8 could not be determined as the responses were too low to fit the curves exactly. Pep1, Pep3, and Pep5 revealed similar association rates of about $1 \cdot 10^5$ (1/M·s). Pep6 showed slightly slower association but also a slower dissociation. However, the dissociation rate k_{off} of Pep3 is the highest k_{off} which is 10-fold more than the dissociation rate of Pep5.

The dissociation constants of the peptides were compared. The tendency of the dissociations constants follows in the order of Pep3 > Pep6 > Pep1 > Pep5, and therefore, the stability or the affinity for the adsorption on TiO_2 can be aligned as Pep5 > Pep1 > Pep6 > Pep3. The maximal response of the peptides correlated with the stability of the adsorption.

3.2. Influence of pH Value and Ionic Strength on the Peptide Adsorption. Investigating the reasons for the strong adsorption of the peptides Pep1, Pep3, Pep5, and Pep6 compared with the other peptides, we determined the influence of the pH and ionic strength on the adsorption on the different materials. The influence of the pH was examined on TiO_2 by SPR measurements. We used buffers with the same ionic strength but different buffer components to achieve pH values of 3, 5, 7, 9, and 11. A direct correlation of the adsorption with the pH value could be found (Figure 4). The adsorption of the peptides increased from pH 3 to 9. The adsorption of Pep1 and Pep3 decreased strongly above pH 9. Pep6 showed a slight decrease for pH 9, while Pep5 adsorbed with constant amounts from pH 7 to 11, but the stability of Pep1, Pep5, and Pep6 considerably decreased at pH 11 as the dissociation constant K_{D} increased (Supporting Information: S-4).

In contrast, the variation of the pH of the buffer from pH 3 to 11 had nearly no effect on the adsorption of Pep2, Pep4, Pep7, and Pep8. The results of the influence of the pH on Pep1 and Pep5 were reproduced on the other materials with fluorescence measurements (Supporting Information: S-5).

The influence of the ionic strength on the peptide adsorption was investigated using PBS pH 7.4 with varied NaCl concentrations. The NaCl concentration of PBS previously used for the adsorption was 154 mM. The influence of the ionic strength was examined with NaCl concentrations in the range

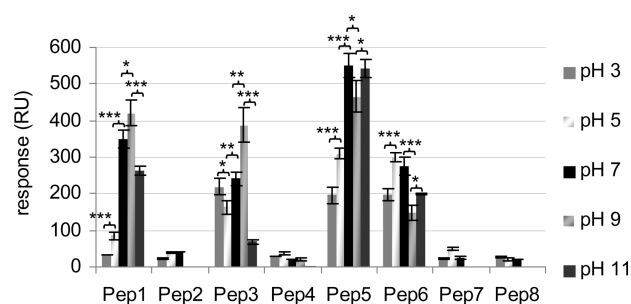


Figure 4. Influence of pH on the peptide adsorption: SPR sensorgrams of the interactions of different peptides Pep1 to Pep8 on TiO_2 at $T = 25$ °C. Sensorgrams were run at the concentration of 1 μM in citrate buffer saline pH 3, acetate buffered saline pH 5, hepes buffered saline pH 7, and borate buffered saline pH 9 and 11 (10 mM buffer, 150 mM NaCl). The flow rate was 30 $\mu\text{L}/\text{min}$. Sample injection was done for 300 s, and desorption phase was 300 s (* $p < 0.05$, ** $p < 0.005$, *** $p < 0.001$).

of 0 to 616 mM. The results determined with fluorescence measurements after desorption for Pep1 are shown in Figure 5.

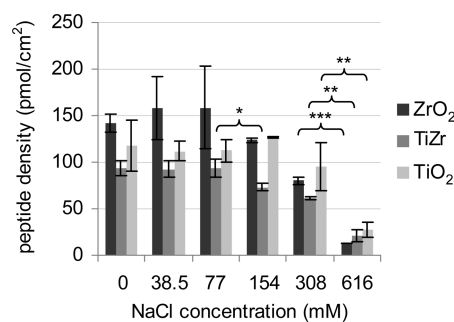


Figure 5. Influence of NaCl concentration. Fluorescence measurements in solution: Surface densities of Pep1Dy557 on ZrO_2 , TiZr , and TiO_2 discs. Adsorption was carried out with 10 μM Pep1 solution in PBS pH 7.4 (0, 38.5, 77, 154, 308, 616 mM NaCl) for 1 h, followed by thorough rinsing of samples and desorption in 5 M NaCl (* $p < 0.05$, ** $p < 0.005$, *** $p < 0.001$).

The influence of the ionic strength showed a decrease of the peptide adsorption with increasing salt concentration for a NaCl concentration higher than 77 mM. For concentrations of 77 mM or lower, no influence was found for neither Pep1 nor Pep5 on each material (Supporting Information: S-6).

3.3. Stability of Peptide Adsorption. The stability of the peptide adsorption on the inorganic materials is important for practical application as anchor molecule. The adsorption has to be stable under different conditions (ionic strength, buffer composition, temperature). To investigate the stability of the peptide adsorption, the ZrO_2 , TiZr , and TiO_2 samples were incubated with the peptides Pep1 and Pep5 under the optimized conditions (10 μM , 1 h), washed, and stored in different media. First, the storage in PBS pH 7.4 was investigated up to 30 d and measured with the enzymatic assay (Figure 6). We proved the adsorption stability of the peptides over 7 d on the materials. Even after 30 d, the peptides could be detected on the ZrO_2 , TiZr , and TiO_2 surfaces at 37 °C.

To show the capability for medical application, the use of cell culture medium (Dulbecco's modified eagle medium (DMEM)) with fetal calf serum (FCS) was examined to simulate *in vivo* conditions. In Figure 7, the surface density after

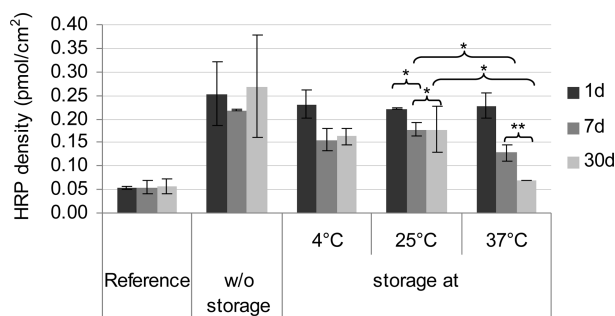


Figure 6. Storage of Pep1 adsorbed on TiO₂ surface at 4, 25, and 37 °C for 1, 7, and 30 d. The adsorption was carried out with 10 μM peptide solution in PBS pH 7.4 for 1 h, stored for different durations, and followed by thorough rinsing of samples.

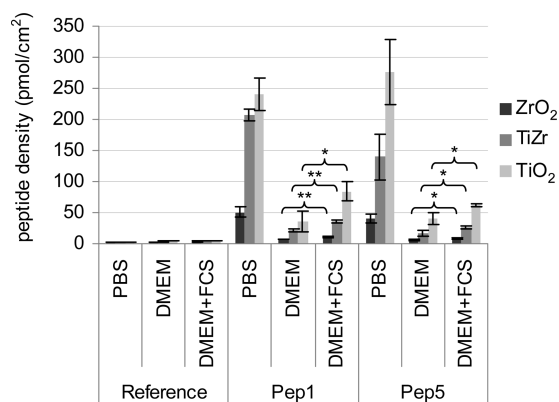


Figure 7. Stability of the peptide adsorption in different media. Fluorescence measurements in solution: Surface densities of Pep1Dy557 and Pep5Dy557 on ZrO₂, TiZr, and TiO₂ discs. Adsorption was carried out with 10 μM peptide solution in PBS pH 7.4 for 1 h, followed by thorough rinsing of samples with PBS and Dulbecco's Modified Eagle Medium (DMEM) with and without fetal calf serum (FCS) for 15 min at room temperature and desorption in 5 M NaCl (* $p < 0.05$, ** $p < 0.005$).

rinsing with buffer and DMEM with and without FCS for 15 min is shown. The peptide densities on the surface were determined after desorption with fluorescence measurements. The experiment revealed a decrease of the peptide density after incubation in DMEM and DMEM with 10% FCS, but still, peptide densities of up to 84 pmol/cm² (Pep1) and 60 pmol/cm² (Pep5) were achieved. The incubation in DMEM without FCS resulted in significant lower peptide densities compared to DMEM with FCS.

3.4. Influence on Human Mesenchymal Stem Cells (hMSCs). The influence of the peptide adsorption on the biocompatibility of the different materials was investigated using hMSCs seeded on ZrO₂, TiZr, and TiO₂ discs with adsorbed Pep5 in comparison to the discs themselves. The proliferation of the hMSCs was measured by determination of the lactate dehydrogenase (LDH) activity in comparison to defined cell counts after 1, 7, and 14 d (Figure 8). 1×10^4 hMSCs per cm² were seeded on the samples with a surface area of 0.196 cm². After 1 d, nearly 2,000 cells were determined on the samples. The cell count doubled after 7 and 14 d each. No significant influence of the different materials and the adsorbed peptide Pep5 could be detected.

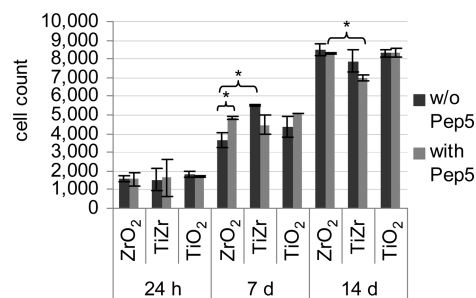


Figure 8. Cell growth on disc-shaped samples with and without adsorbed Pep5: 1×10^4 hMSCs per cm² were seeded, and cell culture medium was added. After 1, 7, and 14 d, the cell count was determined by lactate dehydrogenase (LDH) measurement (* $p < 0.05$).

4. DISCUSSION

4.1. Peptide Selection and Adsorption. The aim of this work was to identify different specific binding peptides for typical implant materials: ZrO₂, TiZr, and Ti, to investigate the adsorption kinetics and to analyze the interactions between the peptides and the materials.

The investigation of the peptide adsorption was proven by a semiquantitative enzymatic assay based on biotin modification of the peptides and interactions with the streptavidin coupled horseradish peroxidase, but the quantitative comparison was not reliable because of the large difference of the activity in solution and immobilized on the disc surface. Additionally, streptavidin offers four binding pockets for biotin and therefore can interact with up to four peptides.

Four of the investigated peptides (Pep1, Pep3, Pep5, and Pep6) could be shown to exhibit a significant and stable adsorption on the relevant materials. Pep2 was found by Sano and Shiba to bind on TiO₂,¹¹ however, we detected only low surface densities of adsorbed Pep2. Possibly, the 3-fold presentation of the binding motif RKLPGA could increase the binding capacity. In this way, Kashiwagi et al. could immobilize BMP-2 on Ti.⁶ Small surface densities were also observed for the phosphoserine containing peptides Pep4, Pep7, and Pep8 at pH 7.4. Accordingly, phosphoserine containing peptides do not seem to be suitable for the modification of oxide surfaces like ZrO₂, TiZr, and TiO₂ under the examined conditions.

Using SPR measurements, we could determine the adsorption kinetics of the peptides on a TiO₂ coated sensor chip. The rating of the peptides was in agreement with the findings of the enzymatic assay. As the adsorption process took place in short periods, the saturation of the surface was achieved within 100 s. The slow desorption process occurred after buffer injection demonstrating the reversibility of the adsorption process. The highest stability of the examined peptides was evaluated for Pep5 (12.3 nM). This K_D value is comparable with antibody–antigen interactions (1 μM to 1 nM, high-affinity antibodies 1 pM) and even higher than most substrate–enzyme interactions (1 mM to 1 μM). The surface densities of the peptides on the SPR chip were estimated via the molecular mass of the peptide and the assumption that 1 RU ≈ 1 pg/mm² and is in the range of 11 pmol/cm² (Pep3), 15 pmol/cm² (Pep6), 24 pmol/cm² (Pep5), and 30 pmol/cm² (Pep1). As this assumption is normally used for purely Au coated sensor chips, the additional coating with TiO₂ might substantially influence this correlation, but these peptide densities should correlate more closely with the actual peptide

densities than the semiquantitative results of the enzymatic assay as the disadvantage of the indirect enzymatic approach with horseradish peroxidase is avoided.

Subsequently, the peptide densities were investigated by fluorescence measurements. Therefore, the peptides with the strongest adsorption (Pep1 and Pep5) were fluorescence labeled and determined after desorption from ZrO₂, TiZr, and TiO₂. Pep1 and Pep5 adsorbed with densities of 70 to 370 pmol/cm². The difference in the peptide density of about a factor of ten between the results of fluorescence and SPR measurements on the TiO₂ surface proves the influence of the increase of the layer thickness or the change in the composition of the layer (from Au to Au with TiO₂) on the SPR measurements. Additionally, the difference in the surface roughness of the samples and the SPR sensor chip might influence the peptide density.

4.1.1. Influence of the Material. The three peptides with the strongest adsorption showed nearly the same behavior on all the materials. These similarities might be caused by the oxide character of the three materials. Ti naturally forms an amorphous oxide layer on the surface (passive layer). TiZr (13–17% Zr) was shown by Wennerberg to form an oxide layer in aqueous solution mainly composed of O (60.4%), Ti (23.4%), Zr (3.5%) and some impurities.¹⁹ They proved the composition of the oxide layer on Ti resembling them on TiZr.

The surface densities of the Pep1 and Pep5 were determined to be in the range of about 70 to 370 pmol/cm² (fluorescence measurements). The surface densities of adsorbed peptides slightly increased from ZrO₂ to TiZr to TiO₂. The differences in the surface densities might be ascribed to surface diversities because of the variable roughness (Supporting Information: S-7). With a higher roughness, the peptide densities increased on the different materials. AFM measurements revealed the average roughness of the TiO₂ discs (6.1 nm) to be higher than TiZr (5.1 nm) and ZrO₂ (1.9 nm). The roughness of the surface influences the specific surface area so that the actual surface of the examined discs is higher than the outer surface used for the determination of the peptide densities. We found a good correlation between the roughness of the materials and the corresponding peptide densities indicating that the peptide density depends on the surface area and not on the kind of material. Additionally, the amount of adsorbed peptides could be further enlarged by an increase in the surface roughness.

4.1.2. Influence of the Peptide Size. The smaller peptide Pep1 (1136.4 g/mol) showed higher surface densities (up to 373 pmol/cm²) than the larger peptide Pep5 (2282.5 g/mol) (up to 316 pmol/cm²) on the three materials indicating a relationship between the size and the surface density. With increasing peptide size, the number of potential binding sites increases and, thus, the part of the surface which is blocked by the peptide adsorption. Additionally, the surface can also be blocked by a peptide with few binding sites but a high molecular weight and thus volume. Therefore, the surface density of the peptides depends on the peptide size and the amount of binding sites, respectively. At the same time, the affinity of the peptide increases with an increasing amount of the binding sites. When a peptide has formed the first interaction, a second interaction of the same peptide is favored compared to another peptide because of the spatial proximity. Accordingly, the stability (K_D) of Pep5 was shown by SPR measurements to be higher on TiO₂ than the stability of Pep1.

4.2. Interactions of Peptides with ZrO₂, TiZr, and TiO₂.

4.2.1. Electrostatic Interaction. The investigated materials

ZrO₂, TiZr, and TiO₂ reveal as already mentioned oxide surfaces. Therefore, they present Ti⁴⁺ and Zr⁴⁺, respectively, as well as O²⁻ binding sites providing the basis for electrostatic interactions. We determined the isoelectric point (IEP) of the materials by zeta potential measurements (Supporting Information: S-8). The IEP for all three materials was 4.5 which might support the explanation for the similar adsorption behavior of the peptides. Thus, the applied pH value of 7.4 results in surfaces with a negative net charge. Attractive electrostatic interactions would take place with positively charged molecules.

In Table 1, the peptide sequences are shown. The composition of the peptides diversifies from partly to completely hydrophilic (Supporting Information: S-9). All peptides, which showed high surface densities (Pep1, Pep3, Pep5, Pep6), reveal mainly hydrophilic amino acids, but there are also peptides consisting mainly of hydrophilic amino acids, which adsorb with no considerably amount (Pep4, Pep7), indicating that the hydrophilic character is important but not the only requirement. Pep1, Pep5, and Pep6 have a high content of neutral and alkaline amino acids (e.g., lysine), and the less adsorbing peptides (Pep4, Pep7, Pep8) have acidic amino acids (phosphoserine) indicating that electrostatic interactions take place between the negatively charged surface and the positively charged alkaline amino acids.

To compare the net charge of the peptides, we determined the isoelectric points (IEP) with isoelectric focusing (Supporting Information: S-10). We found the peptides Pep1, Pep2, Pep5, and Pep6 to have similar IEPs of about 11, and Pep3 had a slightly lower IEP of about 9.5.

The observed strong influence of the pH value on the peptide adsorption supports the assumption that electrostatic interactions play a dominant role. We found a maximum adsorption at about pH 9 for the peptides Pep1 and Pep3 and from pH 7 to 11 for the peptides Pep5 and Pep6. The changes in the charge of the peptides correlated with the adsorption on the samples. Above pH 9, we observed a decrease of the surface density or the stability of the peptide adsorption, respectively. At pH 11, the stability was significantly lower as the peptides are no more positively charged and might repulse the negatively charged materials. At pH values lower than 4.5, the materials become positively charged which results in a repulsion of the positively charged peptides.

The effect of the variation of the NaCl concentration and therewith the ionic strength on the peptide adsorption supports the existence of electrostatic interaction. With an increase in the NaCl concentration, the Pep1 and Pep5 adsorption decreased with concentrations over 154 mM. The higher NaCl concentrations interfere with the electrostatic interactions between the positively charged amino acid residues like lysine and the negatively charged binding sites (O²⁻).

We proved that Pep2, Pep4, Pep7, and Pep8 do not adsorb in high amounts on TiO₂ in the range of pH 3 to 11. Pep2 has an IEP of about 10, but the phosphoserine containing peptides Pep4, Pep7, and Pep8 have IEP of ≤ 2 and 4.5 (Pep8) resulting in negative charges that cause repulsion with the negatively charged surfaces. At lower pH values, both peptides and materials are positively charged. As a result, no significant adsorption of these peptides was found.

4.2.2. Coordinate Interactions. A strong increase of the peptide adsorption from pH 5 to 7 especially of Pep1 and Pep5 was observed by SPR measurements. This increase can not be explained by electrostatic interactions between the Ti⁴⁺ and

Zr⁴⁺ binding sites and the positively charged alkaline amino acids. At pH values higher than 6, the histidine groups are deprotonated. The change of the pH value from 5 to 7 decreases the positive charge of the peptides and thereby the attractive electrostatic interactions. However, we found an increase of the adsorption which can be explained by coordinate interactions.

Coordinate interactions could take place between Ti⁴⁺, Zr⁴⁺ and Ti–OH₂⁺, Zr–OH₂⁺, respectively, and the deprotonated nitrogen atom of the histidine residue. Liao calculated the intensity of histidine interactions with other molecules.²⁰ They found the coordinate interactions between the neutral histidine and metallic cations to be the strongest interaction of histidine and estimated an interaction energy of –8.6 kcal/mol for the imidazole–Ca²⁺ interaction and –16.8 kcal/mol for the imidazole–Zn²⁺ interaction in water (B3LYP with PCM method).

4.2.3. Hydrogen Bonds. Further interactions of the peptides with ZrO₂, TiZr, and TiO₂ might be hydrogen bonds of the amino acids via amino groups (e.g., arginine, lysine) or hydroxyl groups (e.g., serine, threonine) and the O^{2–} binding sites. The existence of hydrogen bonds can be supported by the adsorption of the peptides Pep1, Pep3, Pep5, and Pep6 at pH 3 and 11. Although electrostatic interactions can be ruled out at these pH values, we found significant adsorption. The deprotonated histidine and lysine residues as well as the serine residue might form hydrogen bonds with the Ti–OH₂⁺ and Zr–OH₂⁺ binding sites resulting in the observed adsorption.

4.2.4. Hydrophobic Interaction. Hydrophobic interaction as the reason for the adsorption of the different peptides on the investigated materials can almost be excluded because of the low hydrophobicity of ZrO₂, TiZr, and TiO₂ exhibiting an oxide character. Analyzing the amino acid content of the peptides, which adsorb stably and with high surface densities, we did not reveal many hydrophobic amino acids. Pep3 exhibits 28% hydrophobic amino acids (valine, methionine, proline, and phenylalanine). However, Pep1, Pep5 and Pep6 contain zero and one, respectively, hydrophobic amino acid (proline). Therefore, hydrophobic interactions seem to not contribute to the peptide adsorption on the given material surfaces.

4.2.5. Peptide Conformation and Sequence. Another important parameter for the adsorption is the conformation of the peptide. Chen et al. identified the lysine residues of Pep1 as essential for the adsorption on TiO₂.²¹ The three lysine residues were found to be orientated toward the TiO₂ surface. A higher lysine content decreased the adsorption as the conformation became more rigid because of intramolecular repulsion. Krauland et al. investigated lysine containing peptides on α -Al₂O₃ and found the separated lysine residues to have a more favorable influence on the adsorption than grouped lysine residues.²² Especially, Pep5 and Pep6 reveal this favorable separation of the lysine residues.

4.3. Applicability of the Peptides for Medical Implants. For medical application, the immobilization systems on the implant surface have to fulfill different requirements: (i) high stability at human body temperature, (ii) stability against components of blood, and (iii) compatibility with surrounding cells and tissues. The requirements (i) and (ii) were examined by the determination of the peptide density after the incubation of the modified samples at different temperatures, at different durations, and in different media. The comparison before and after the incubation allows for conclusions about the stability of the peptides on the sample surface.

The stability of the peptides on the three materials could be proven up to 30 d at 4, 25, and 37 °C. At 37 °C, the peptide density decreased during 30 d but peptides remained on the samples which allows for biomedical application of the anchor peptides. This is especially important for the immobilization of growth factors like the vascular endothelial growth factor (VEGF) or bone morphogenetic proteins (BMPs).

We investigated (ii) the peptide stability against components of the blood by the incubation with the cell culture media DMEM with and without FCS. Under these conditions, the peptide density decreased. However, peptide densities up to 84 pmol/cm² were still obtained. Therefore, the stability could be proven in the competition with, e.g., other peptides and proteins. This provides the basis for the investigation of (iii) the compatibility with surrounding cells. The cultivation of hMSCs in cell culture media on the disc-shaped samples with peptide Pep5 was investigated. After 24 h, the adhesion of all of the seeded cells was proven on the samples. The proliferation of the hMSCs on ZrO₂, TiZr, and TiO₂ samples with and without Pep5 showed the same results for up to 14 d. Therewith, we identified Pep5 as promising anchor peptide for the stable immobilization of biologically active molecules in satisfying amounts.

5. CONCLUSION

In this work, we investigated eight peptides selected from the literature as anchor peptides to adsorb on the typical implant materials ZrO₂, TiZr, and Ti/TiO₂. Four of the eight peptides (Pep1, Pep3, Pep5, and Pep6) were found to adsorb in large amounts with surface densities of up to 370 pmol/cm². The kinetics of the peptide adsorption measured with surface plasmon resonance measurements exhibit a fast and stable adsorption with dissociation constants of up to 12.3 nM (Pep5). The long-term stability was investigated over a time period of 30 d at 4, 25, and 37 °C. From these investigations, including the effect of the ionic strength, we conclude that the interaction between the selected peptides and the inorganic materials ZrO₂, TiZr, and TiO₂ is mostly driven by different weak interactions with the order of electrostatic interactions > coordinate interactions > hydrogen bonds. In competition with proteins from cell culture media, there was a decrease of the surface density of the peptides, but still, densities of up to 84 pmol/cm² could be reached. The peptides adsorbed on the samples did not have any effect on the adhesion or proliferation of human mesenchymal stem cells. Therefore, the anchor peptides are suitable candidates for medical application. Pep5 showed the most stable adsorption and thus is a promising anchor for biologically active molecules (e.g., RGD peptides, antibiotics, or growth factors) for the improvement of the incorporation of implants, particularly in the case of patients with risk factors like smoking or osteoporosis.

■ ASSOCIATED CONTENT

Supporting Information

S-1: Influence of the peptide concentration on the peptide adsorption of Pep1, Pep3, Pep5, Pep6, and Pep7 on ZrO₂; S-2: Influence of the incubation time on the peptide adsorption of (a) Pep1, (b) Pep5, and (c) Pep6 on ZrO₂, TiZr, and TiO₂; S-3: Influence of the peptide concentration on the peptide adsorption; S-4: Influence of pH value on the peptide adsorption, dissociation constants K_D derived from SPR sensorgrams of the interactions of the peptides Pep1, Pep3, Pep5, and Pep6 on TiO₂; S-5: Influence of pH value on the

Pep1 and Pep5 adsorption on ZrO₂ and TiZr; S-6: Influence of NaCl concentration on the Pep5Dy557 adsorption on ZrO₂, TiZr, and TiO₂; S-7: Roughness average R_a (arithmetic average of absolute values) of ZrO₂, TiZr, and TiO₂ samples determined with AFM measurements; S-8: Zetapotential Measurements of ZrO₂, TiZr, and TiO₂; S-9: Amino acid content of the examined peptides: (a) Percentage hydrophobic and hydrophilic amino acids. (b) Percentage neutral, alkaline, and acidic amino acids; S-10: Isoelectric focusing (IEF), nonequilibrium pH gel electrophoresis (NEPHGE) of the peptides Pep1, Pep2, Pep3, Pep5, and Pep6. This material is available free of charge via the Internet at <http://pubs.acs.org>.

AUTHOR INFORMATION

Corresponding Author

*E-mail: Dieter.Scharnweber@tu-dresden.de. Phone: +49-351-463 39379. Fax: +49-351-463 39401.

Author Contributions

‡D.S. and B.S. contributed equally.

Notes

The authors declare no competing financial interest.

ACKNOWLEDGMENTS

The authors would like to thank the ITI for providing financial support (ITI Research Grant No. 680_2010). We want to thank Institute Straumann AG, Basel, for providing materials. We thank Dr. Christian Wenzel and Ulrich Merkel at the Department of Semiconductor Technology, TU Dresden, for titanium coating of the SPR sensor chips and Dr. Vera Hintze at the Max Bergmann Center of Biomaterials, TU Dresden, for the provision of the BIAcore T100 instrument. We thank Dr. Cornelia Bellmann and Anja Caspari at the IPF Dresden for performing the zeta potential measurements.

REFERENCES

- (1) Ooka, A.; Garrell, R. L. Surface-Enhanced Raman Spectroscopy of DOPA Containing Peptides Related to Adhesive Protein of Marine Mussel, *Mytilus Edulis*. *Biopolymers* **2000**, *57*, 92–102.
- (2) Dalsin, J. L.; Hu, B.-H.; Lee, B. P.; Messersmith, B. P. Mussel Adhesive Protein Mimetic Polymers for the Preparation of Nonfouling Surfaces. *J. Am. Chem. Soc.* **2003**, *125*, 4253–4258.
- (3) Lee, H.; Lee, B. P.; Messersmith, B. P. A Reversible Wet/Dry Adhesive Inspired by Mussels and Geckos. *Nature* **2007**, *448*, 338–342.
- (4) Yu, M.; Hwang, J.; Deming, T. J. Role of L-3,4-Dihydroxyphenylalanine in Mussel Adhesive Proteins. *J. Am. Chem. Soc.* **1999**, *121*, 5825–5826.
- (5) Kacar, T.; Zin, M. T.; So, C.; Wilson, B.; Ma, H.; Gul-Karaguler, N.; Jen, A. K.-Y.; Sarikaya, M.; Tamerler, C. Directed Self-Immobilization of Alkaline Phosphatase on Micro-Patterned Substrates via Genetically Fused Metal-Binding Peptide. *Biotechnol. Bioeng.* **2009**, *103*, 696–705.
- (6) Kashiwagi, K.; Tsuji, T.; Shiba, K. Directional BMP-2 for Functionalization of Titanium Surfaces. *Biomaterials* **2009**, *30*, 1166–1175.
- (7) Meyers, S. R.; Khoo, X.; Huang, X.; Walsh, E. B.; Grinstaff, M. W.; Kenan, D. J. The Development of Peptide-Based Interfacial Biomaterials for Generating Biological Functionality on the Surface of Bioinert Materials. *Biomaterials* **2009**, *30*, 277–286.
- (8) Razvag, Y.; Gutkin, V.; Reches, M. Probing the Interaction of Individual Amino Acids with Inorganic Surfaces Using Atomic Force Spectroscopy. *Langmuir* **2013**, *29*, 10102–10109.
- (9) Chen, H.; Su, X.; Neoh, K.-G.; Choe, W.-S. QCM-D Analysis of Binding Mechanism of Phage Particles Displaying a Constrained Heptapeptide with Specific Affinity to SiO₂ and TiO₂. *Anal. Chem.* **2006**, *78*, 4872–4879.
- (10) Chen, H.; Su, X.; Neoh, K.-G.; Choe, W.-S. Context-Dependent Adsorption Behavior of Cyclic and Linear Peptides on Metal Oxide Surfaces. *Langmuir* **2009**, *25*, 1588–1593.
- (11) Sano, K.; Shiba, K. A Hexapeptide Motif that Electrostatically Binds to the Surface of Titanium. *J. Am. Chem. Soc.* **2003**, *125*, 14234–14235.
- (12) Gronewold, T. M. A.; Baumgartner, A.; Weckmann, A.; Knekties, J.; Egler, C. Selection Process Generating Peptide Aptamers and Analysis of Their Binding to the TiO₂ Surface of a Surface Acoustic Wave Sensor. *Acta Biomater.* **2009**, *5*, 794–800.
- (13) Khoo, X.; Hamilton, P.; O'Toole, G. A.; Snyder, B. D.; Kenan, D. J.; Grinstaff, M. W. Directed Assembly of PEGylated-Peptide Coatings for Infection-Resistant Titanium Metal. *J. Am. Chem. Soc.* **2009**, *131*, 10992–10997.
- (14) Larsen, M. R.; Thingholm, T. E.; Jensen, O. N.; Roepstorff, P.; Jorgensen, T. J. D. Highly Selective Enrichment of Phosphorylated Peptides from Peptide Mixtures Using Titanium Dioxide Microcolumns. *Mol. Cell. Proteomics* **2005**, *4*, 873–886.
- (15) Zhou, H.; Tian, R.; Ye, M.; Xu, S.; Feng, S.; Pan, C.; Jiang, X.; Li, X.; Zou, H. Highly Specific Enrichment of Phosphopeptides by Zirconium Dioxide Nanoparticles for Phosphoproteome Analysis. *Electrophoresis* **2007**, *28*, 2201–2215.
- (16) Bisswanger, H. *Practical Enzymology*; Wiley: Weinheim, 2004; pp 80.
- (17) Gaebler, A.; Schaefer, T.; Fischer, K.; Scharnweber, D.; Mauth, C.; Schwenzer, B. Peptide Linkers for the Immobilization of Bioactive Molecules on Biphasic Calcium Phosphate via a Modular Immobilization System. *Acta Biomater.* **2013**, *9*, 4899–4905.
- (18) Atkins, P. W. *Physikalische Chemie*; Wiley: Weinheim, 2001.
- (19) Wennerberg, A.; Svanborg, L. M.; Berner, S.; Andersson, M. Spontaneously Formed Nanostructures on Titanium Surfaces. *Clin. Oral Implants Res.* **2012**, *24*, 203–209.
- (20) Liao, S.-M.; Du, Q.-S.; Meng, J.-Z.; Pang, Z.-W.; Huang, R.-B. The Multiple Roles of Histidine in Protein Interactions. *Chem. Cent. J.* **2013**, *7*, 1–12.
- (21) Chen, H.; Su, X.; Neoh, K.-G.; Choe, W.-S. Probing the Interaction between Peptides and Metal Oxides Using Point Mutants of a TiO₂-Binding Peptide. *Langmuir* **2008**, *24*, 6852–6857.
- (22) Krauland, E. M.; Peelle, B. R.; Wittrup, K. D.; Belcher, A. M. Peptide Tags for Enhanced Cellular and Protein Adhesion to Single-Crystalline Sapphire. *Biotechnol. Bioeng.* **2007**, *97*, 1009–1020.